Inorg. Chem. **2004**, *43*, 2793–2802

A Systematic Evaluation of Molecular Recognition Phenomena. 4. Selective Binding of Dicarboxylic Acids to Hexaazamacrocyclic Ligands Based on Molecular Flexibility

Carmen Anda,[†] Antoni Llobet,*[,†] Arthur E. Martell,[‡] Joseph Reibenspies,[‡] Emanuela Berni,[§] and Xavier Solans[||]

Departament de Química, Universitat de Girona, Campus de Montilivi, E-17071 Girona, Spain, Department of Chemistry, Texas A&M University, College Station, Texas 77843-3255, Department of Chemistry, University of Florence, Via della Lastruccia 3, I50019 Sesto Fiorentino, Florence, Italy, and Departament de Cristal·lografia, Mineralogia i Dipòsits Minerals, Universitat de Barcelona, Martí i Franquès, s/n, E-08028 Barcelona, Spain

Received September 24, 2003

The host–guest interaction between four hexaaza macrocyclic ligands (3,6,9,17,20,23-hexaazatricyclo[23.3.1.1^{11,15}]-triaconta-1(29),11,13,15 (30),25(27)-hexaene (Bd), 3,6,9,16,19,22-hexaazatricyclo[22.2.2.2^{11,14}]triaconta-1(27),11-(30),12,14(29),24(28),25-hexaene (P2), 3,7,11,19,23,27-hexaazatricyclo[27.3.1.1^{13,17}]tetratriaconta-1(33),13, 15,17-(34),29,31-hexaene (Bn), 3,7,11,18,22,26-hexaazatricyclo[26.2.2.2^{13,16}]tetratriaconta-1(31),13(34),14,16(33),28(32),29-hexaene (P3)) and two dicarboxylic acids (oxalic acid, H_2Ox; oxydiacetic acid, H_2Od) have been investigated using potentiometric equilibrium methods. Ternary complexes are formed in aqueous solution as a result of hydrogen bond formation and Coulombic interactions between the host and the guest. In the $[(H_6P2)(Ox)]^{4+}$ complex those bonding interactions reach a maximum yielding a log K^R_6 of 6.08. This species has been further characterized by means of X-ray diffraction analysis showing that the oxalate guest molecule is situated inside the macrocyclic cavity of the P2 host. X-ray diffraction analysis has also been carried out for the complex $[(H_6Bn)(Od)_2](Br)_2 \cdot 6H_2O$, where now the oxydiacetate is bonded to the host but outside the macrocyclic cavity. Competitive distribution diagrams and total species distribution diagrams are used to graphically illustrate the most salient features of these systems, which are the following: (a) The Bd and P2 ligands bind Ox significantly much more stronger than Od. This is clearly manifested for the P2:Ox:Od competitive system, where a selectivity of 92.5% in favor of the P2–Ox complexation against P2–Od is obtained at p[H] = 2.8. (b) No isomeric effect is found when comparing binding capacities of oxalate with two isomeric ligands such as P2 and Bd since their affinity to bind the substrate is relatively similar. (c) Bn and P3 ligands have a similar behavior as described in (a) for P2 and Bd except that due to the increase of cavity size the differentiation becomes smaller. (d) Less basic ligands containing two methylenic units Bd (log β^H_6 = 40.42) and P2 (40.42) bind stronger to the substrates than those containing three methylenic units Bn (50.32) and P3 (50.64) even though their relative predominance depends on p[H].

Introduction

The molecular recognition of anionic guest species is an area of current intense chemical investigation with potential applications in environmental, industrial, and health-related disciplines.[1]

Within this field, we have recently undertaken a systematic evaluation of molecular recognition phenomena between phosphates and nucleotides based on hexaazamacrocyclic ligands containing xylylic and diethylic ether spacers.[2] In this work, we have quantitatively evaluated the different factors involved in the recognition processes, namely, geometric fit, Coulombic interactions, hydrogen bonding, and $\pi-\pi$ stacking interactions.

We are now directing our attention to the coordination of dicarboxylic substrates[3] given their multiple and important

* Author to whom correspondence should be addressed. E-mail: antoni.llobet@udg.es.
[†] Universitat de Girona.
[‡] Texas A&M University.
[§] University of Florence.
[||] Universitat de Barcelona.

10.1021/ic035121p CCC: $27.50
Published on Web 03/17/2004

implications in biological processes;[1] for instance, hyperoxaluria is an illness caused by excessive generation and excretion of oxalate. It is also well documented that excess of oxalate anion, a minor constituent in ordinary foodstuffs, can cause serious damage to bone tissue. For these reasons it is of special interest to design oxalate receptors that (a) can allow to built up sensors for monitoring purposes and (b) can permit its sequestration.[3a]

In this paper we report the host−guest binding interactions of a family of four ditopic hexaazamacroyclic ligands containing *meta*- and *para*-xylylic spacers and different content of methylenic units within amine groups as shown in the Chart 1. These four ligands allow us to perform a systematic evaluation of the fundamental features involved in host−guest binding interactions with different dicarboxylic acids, including the geometrical fit, which is described here on.

Experimental Section

Materials. RG grade KCl was obtained from Aldrich, and CO_2-free Dilut-it ampules of KOH were purchased from J. T. Baker Inc. Reagent grade oxydiacetic and oxalic acids were purchased from Merck. The KOH solution was standardized by titration against standard potassium acid phthalate with phenolphthalein as indicator and was checked periodically for carbonate content (<2%).[4] Ligands Bd, P2, Bn, and P3 (see Chart 1 for abbreviations used) have been synthesized and characterized according to previously published procedures.[2c,5−8]

Chart 1. Drawings and Abbreviations for the Ligands and Substrates

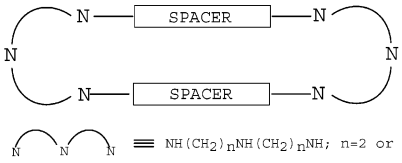

Ligand	Spacer	n	Cavity[a]	Basicity
Bd		2	1.00	40.42
P2		2	1.12	40.42
Bn		3	1.20	50.32
P3		3	1.34	50.64

[a] Cavity size normalized for the smallest mac Bd (see text)

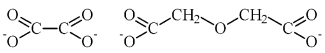

Ox Od

Potentiometric Titrations. Potentiometric measurements were conducted in a jacketed cell thermostated at 25.0 °C and kept under an inert atmosphere of purified and humidified argon. For the potentiometric measures a Crison pHmeter, (model 2002) was used equipped with a glass electrode and a Ag/AgCl reference electrode with saturated KCl as internal solution. The volume of titrating agent to be added to the reaction mixture was controlled by means of a electronic Crison buret with a nominal volume of 2.5 mL. The support electrolyte used to keep ionic strength constant at 0.10 M was KCl. The electrodes were calibrated by titrating a small amount of HCl at an ionic strengh of 0.10 M and a constant temperature of 25 °C and determining the titration end point with the Gran[9] method that allows one to calculate the electrode's standard potential ($E°$). log K_w for the system, defined in terms of log($[H^+][OH^-]$), was found to be −13.78 at the ionic strength employed[10] and was kept fixed during refinements.

Acid dissociation constants for the oxalic acid and oxydiacetic acid were determined under exact conditions employed in this work and were found to agree well with data from the literature.[10]

Potentiometric measurements of solutions either containing the ligand or the ligand plus equimolecular amounts the appropriate substrate were run at concentrations of 2.0×10^{-3} M and ionic strengths of $\mu = 0.10$ M (KCl). At least 10 points/neutralization of every hydrogen ion equivalent were acquired, repeating titrations until satisfactory agreement was obtained. A minimum of three consistent set of data were used in each case to calculate the overall stability constants and their standard deviations. The range of accurate p[H] measurements were considered to be 2−12. Equilibrium constants and species distribution diagrams were calculated using the programs BEST[11] and SPEXY, respectively.[12]

NMR Spectroscopy. ^{1}H NMR spectra in D_2O solution at different pH values were recorded at 298 K in a Varian 300 MHz spectrometer. The peak positions are reported relative to HOD at

(1) (a) Mason, S.; Clifford, T.; Seib, L.; Kuczera, K.; Bowman-James, K. *J. Am. Chem. Soc*. **1998**, *120*, 8890−8900. (b) Sun, S.-S.; Lees, A. J.; Zavalij, P. Y. *Inorg. Chem*. **2003**, *42*, 3445−3453. (c) Tobey, S. L.; Jones, B. J.; Anslyn, E. V. *J. Am. Chem. Soc*. **2003**, *125*, 4026−4027. (d) Tobey, S. L.; Anslyn, E. V. *Organic Lett.* **2003**, *5*, 2029−2031. (e) Cutland, A. D.; Halfen, J. A.; Kampf, J. W.; Pecoraro, V. L. *J. Am. Chem. Soc*. **2001**, *123*, 6211−6212. (f) Choi, K.; Hamilton, A. D. *J. Am. Chem. Soc*. **2001**, *123*, 2456−2457. (g) Lee, D. H.; Im, J. H.; Son, S. U.; Chung, Y. K.; Hong, J.-I. *J. Am. Chem. Soc.* **2003**, *125*, 7752−7753. (h) Bernhardt, P. V.; Hayes, E. J. *Inorg. Chem*. **2003**, *42*, 1371−1377. (i) Lee, C.-H.; Yoon, D.-W.; Won, D.-H.; Cho, W.-S.; Lynch, V. M.; shevchuk, S. V.; Sessler, J. L. *J. Am. Chem. Soc*. **2003**, *125*, 7301−7306. (j) Otto, S.; Kubik, S. *J. Am. Chem. Soc*. **2003**, *125*, 7804−7805. (k) Tomapatanaget, B.; Tuntulani, T.; Chailapakul, O. *Organic Lett.* **2003**, *5*, 1539−1542. (l) Kacprzak, K.; Gawronski, J. *Chem. Commun*. **2003**, 1532−1533.

(2) (a) Anda, C.; Llobet A.; Salvadó, V.; Reibenspies, J.; Martell, A. E.; Motekaitis, R. J. *Inorg. Chem*. **2000**, *39*, 2986. (b) Anda, C.; Llobet, A.; Salvadó, V.; Martell, A. E.; Motekaitis, R. J. *Inorg. Chem*. **2000**, *39*, 3000. (c) Anda, C.; Llobet, A.; Martell, A. E.; Donnadieu, B. *Inorg. Chem*. **2003**, *42*, 8385.

(3) (a) Nelson, J.; Nieuwenhuyzen, M.; Pál, I.; Town, R. M. *Chem. Commun*. **2002**, 2266−2267. (b) Bazzicalupi, C.; Bencini, A.; Bianchi, A.; Fusi, V.; García-España, E.; Giorgi, C.; Llinares, J. M.; Ramírez, J. A.; Valtancoli, B. *Inorg. Chem*. **1999**, *38*, 620−621. (c) Rebek, J., Jr.; Nemeth, D.; Ballester, P.; Lin, F. T. *J. Am. Chem. Soc*. **1987**, *109*, 3474−3475. (d) Tanaka, Y.; Kato, Y.; Aoyama, Y. *J. Am. Chem. Soc*. **1990**, *112*, 2807−2808. (e) Lu, Q.; Motekaitis, R. J.; Reibenspies, J. J.; Martell, A. E. *Inorg. Chem.* **1995**, *34*, 4958−4963. (f) Zafar, A.; Melendez, R.; Geib, S. J.; Hamilton, A. D. *Tetrahedron* **2002**, *58*, 683−690. (g) Linton, B. R.; Goodman, M. S.; Fan, E.; Arman, S. C.; Hamilton, A. D. *J. Org. Chem*. **2001**, *66*, 7313−7319. (h) Sansone, F.; Baldini, L.; Casnati, A.; Lazzarotto, M.; Ugozzoli, F.; ungaro, R. *Proc. Natl. Acad. Sci. U.S.A.* **2002**, *99*, 4842−4847. (i) goswami, S.; Ghosh, K.; Dasgupta, S. *J. Org. Chem*. **2000**, *65*, 1907−1914.

(4) Martell, A. E.; Motekaitis, R. J. *Determination and Use of Stability Constants*, 2nd ed.; John Wiley and Sons: New York, 1992.

(5) Menif, R.; Martell, A. E. *J. Chem. Soc., Chem. Commun*. **1989**, 1522.

(6) Llobet, A.; Reibenspies, J.; Martell, A. E. *Inorg. Chem*. **1994**, *33*, 5946.

(7) Chen, D.; Martell, A. E. *Tetrahedron* **1991**, *47*, 689.

(8) Pietraszkiewiez, M.; Gasiorowski, R. *Chem. Ber*. **1990**, *123*, 405.

(9) Gran, G. *Analyst (London)* **1952**, *77*, 661.

(10) Smith, R. M.; Martell, A. E. *NIST Critically Selected Stability Constants: Version 2.0*; National Institute of Standards and Technology: Gaithersburg, MD, 1995.

(11) Martell, A. E.; Motekaitis, R. J. *Determination and Use of Stability Constants*, 2nd ed.; John Wiley and Sons: New York, 1992.

(12) SPEXY is a program created by R. J. Motekaitis which generates an *X*−*Y* file that contains the concentration of all the existent species in solution as a function of p[H] using BEST output files.

4.79 ppm. Small amounts of 0.01 mol·dm^{-3} NaOD or DCl solutions were added to a solution of the ligand to adjust the pD. The pH was calculated from the measured pD values using the following relationship: pH = pD − 0.40.[13]

Preparation of Crystalline Complexes. [(H_6P2)(Ox)]Br_4·4H_2O, 1. A solution of 0.05 mmol of disodium oxalate in 2 mL of water was added dropwise over a solution of 0.046 mmol of the ligand [H_6P2]Br_6 in 2 mL of water. After 2 weeks of a slow diffusion of this solution with ethanol at room temperature, appropriate crystals for X-ray diffraction were obtained.

[(H_6Bn)(Od)$_2$]Br_2·6H_2O, 2. A solution of 0.21 mmol of oxydiacetic acid in 1 mL of water was added dropwise over a solution of 0.100 mmol of the ligand [H_6Bn]Br_6 in 3 mL of water. The pH was adjusted to 5.0 by addition of small amounts of a 0.1 M solution of NaOH. The solution was allowed to evaporate at room temperature, and after 1 week, appropriate crystals for X-ray diffraction were obtained.

Crystal Structure Determinations. [(H_6P2)(Ox)]Br_4·2H_2O. A prismatic crystal (0.1 × 0.1 × 0.2 mm) was selected and mounted on a MAR345 diffractometer with image plate detector. Unit cell parameters were determined from automatic centering of 2607 reflections ($2 < \theta < 27$) and refined by the least-squares method. Intensities were collected with graphite-monochromatized Mo Kα radiation. A total of 10 041 reflections were measured in the range $1.89 \le \theta \le 26.73$, 3735 of which which nonequivalent by symmetry (R_{int} (on I) = 0.031). A total of 2313 reflections were assumed as observed by applying the condition $I > 2\sigma(I)$. Lorentz−polarization and absorption corrections were made.

The structure was solved by direct methods, using the SHELXS computer program[14] and refined by the full-matrix least-squares method with the SHELX97 computer program,[14] using 2916 reflections (very negative intensities were not assumed). The function minimized was $\{\sum w||F_o|^2 - |F_c|^2|$, where $w = [\sigma^2(I) + (0.0421P)^2 + 4.3801P]^{-1}$ and $P = (|F_o|^2 + 2|F_c|^2)/3$. f, f', and f'' were taken from ref 15. A total of 26 H atoms were located from a difference synthesis and refined with an overall isotropic temperature factor. The final R (on F) factor was 0.039, wR (on $|F|^2$) = 0.095, and goodness of fit = 1.103 for all observed reflections. The number of refined parameters was 297. Maximum shift/esd = 0.00. The maximum and minimum peaks in final difference synthesis were 0.503 and −0.480 e Å^{-3}, respectively.

Drawings of molecules are performed with the program ORTEP32[16] with 50% probability displacement ellipsoids for nonhydrogen atoms.

[(H_6Bn)(Od)$_2$]·6H_2O. A Bausch and Lomb 10× microscope was used to identify a suitable colorless needle 0.3 mm × 0.02 mm × 0.02 mm from a representative sample of crystals of the same habit. The crystal was coated in a cryogenic protectant (Paratone) and was then fixed to a glass fiber which in turn was fashioned to a copper mounting pin. The mounted crystal was then placed in a cold nitrogen stream (Oxford) maintained at 110 K.

A Bruker SMART 1000 X-ray three-circle diffractometer was employed for crystal screening, unit cell determination, and data collection.The goniometer was controlled using the SMART software suite, version 5.056 (Microsoft NT operating system). The sample was optically centered with the aid of a video camera such that no translations were observed as the crystal was rotated through all positions. The detector was set at 5.0 cm from the crystal sample (CCD-PXL-KAF2, SMART 1000, 512 × 512 pixel). The X-ray radiation employed was generated from a Mo-sealed X-ray tube (Kα = 0.701 73 Å with a potential of 50 kV and a current of 40 mA) and filtered with a graphite monochromator in the parallel mode (175 mm collimator with 0.5 mm pinholes).

Dark currents were obtained for the appropriate exposure time 10 s, and a rotation exposure was taken to determine crystal quality and the X-ray beam intersection with the detector. The beam intersection coordinates were compared to the configured coordinates, and changes were made accordingly. The rotation exposure indicated acceptable crystal quality, and the unit cell determination was undertaken. A total of 60 data frames were taken at widths of 0.3° with an exposure time of 10 s. Over 50 reflections were centered, and their positions were determined. These reflections were used in the autoindexing procedure to determine the unit cell. A suitable cell was found and refined by nonlinear least squares and Bravais lattice procedures and reported here in Table 1. The unit cell was verified by examination of the *hkl* overlays on several frames of data, including zone photographs. No supercell or erroneous reflections were observed.

After careful examination of the unit cell, a standard data collection procedure was initiated. This procedure consists of collection of one hemisphere of data collected using ω scans, involving the collection 1201 0.3° frames at fixed angles for ϕ, 2θ, and χ ($2\theta = -28°$, $\chi = 54.73°$), while varying ω. Each frame was exposed for 20 s and contrasted against a 20 s dark current exposure. The total data collection was performed for duration of approximately 13 h at 110 K. No significant intensity fluctuations of equivalent reflections were observed.

After data collection, the crystal was measured carefully for size, morphology, and color. These measurements are reported in Table 1.

Table 1. Summary of Crystal Structure Results for the Complexes

param	[(H_6P2)(Ox)](Br_4·4H_2O **(1)**	[(H_6Bn)(Od)$_2$](Br_2·6H_2O **(2)**
empirical formula	$C_{26}H_{54}N_6O_8Br_4$	$C_{36}H_{72}N_6O_{16}Br_2$
M_r	898.39	1004.82
cryst system	monoclinic	triclinic,
space group	$P2_1/n$	$P\bar{1}$
a (Å)	7.6990(10)	10.460(5)
b (Å)	18.0200(10)	11.650(5)
c (Å)	13.589(3)	12.115(6)
α (deg)		74.22(2)
β (deg)	98.82(2)	65.170(10)
δ (deg)		68.070(10)
V (Å^3)	1863.0(5)	1231.2(10))
Z	2	1
temp (K)	296(2)	162(2)
λ(Mo Kα) (Å)	0.710 69	0.710 69
ρ (g/cm^3)	1.602	0.71073
μ (mm^{-1})	4.370	0.104
R [$I > 2\sigma(I)$][a]	0.0399	0.0685
wR (all data)[b]	0.0954	0.1605

[a] $R = \sum||F_o| - |F_c||/\sum|F_o|$. [b] $wR = [\sum[w(F_o^2 - F_c^2)^2/\sum[w(F_o^4)]]^{1/2}$.

Results and Discussion

Solid-State Structure of 1 and 2. Mixing equimolecular amounts of [H_6P2]Br_6 and disodium oxalate in water generates colorless crystals of [(H_6P2)(Ox)]Br_4·2H_2O, **1**, after a slow diffusion of this solution with ethanol at room temperature. [(H_6Bn)(Od)$_2$]Br_2·6H_2O, **2**, is prepared by

(13) Covington, A. K.; Paabo M., Robinson, R. A. Bates, R. G. *Anal. Chem.* **1968**, *40*, 700.
(14) Sheldrick, G. M. *SHELXL97. A computer program for determination of crystal structure*; University of Göttingen: Göttingen, Germany, 1997.
(15) *International Tables for X-ray Crystallography*; Kynoch Press: Birmingham, U.K., 1974; Vol. IV, pp 99−100 and 149.
(16) ORTEP3 for Windows: Farrugia, L. J. *J. Appl. Crystallogr*. **1997**, *30*, 565.

Table 2. Hydrogen Bond Metric Parameters (Å, deg) for Anionic Complexes **1** and **2**

compd **1**[a] D−H···A	*d*(D−H)	*d*(H···A)	*d*(D···A)	∠(DHA)
N1−H1na···Br1	0.94(6)	2.27(7)	3.185(4)	164(5)
N1−H1n···O4	0.79(5)	2.43(5)	2.971(6)	127(5)
N1−H1n···O3	0.79(5)	2.31(5)	2.977(6)	143(5)
N2−H2na···O2	0.98(5)	1.82(5)	2.789(5)	174(5)
N2−H2n···Br2_4	0.87(5)	2.44(5)	3.304(4)	176(5)
N3−H3n···O4	0.8996[b]	1.9111[b]	2.796(6)	167.45[b]
N3−H3na···O1_3	0.9003[b]	1.9435[b]	2.795(5)	157.05[b]
N3−H3na···O2	0.9003[b]	2.4669[b]	3.097(5)	127.34[b]
O3−H3oa···O1	0.72(5)	2.12(5)	2.828(6)	169(6)
O3−H3o···O2	0.82(6)	1.96(6)	2.753(5)	164(5)
O4−H4o···Br2	0.73(7)	2.49(7)	3.210(5)	170(7)
O4_3-H4oa_3···Br1	0.74(7)	2.54(7)	3.265(5)	166(7)

compd **2**[c] D−H···A	*d*(D−H)	*d*(H···A)	*d*(D···A)	∠(DHA)
N1−H1a···O5_2	0.92	2.013	2.809	143.97
N1−H1d···O1_2	0.920	1.795)	2.708	171.24
N2−H2a···O1	0.919	2.400	3.061	128.76
N2−H2d···O5	0.920	1.883	2.797	172.00
N2−H2a···O2	0.919	1.942	2.826	160.67
N2−H2d···O4	0.920	2.710	3.239	117.49
N3−H3a···O2_2	0.921	1.822	2.708	160.66
N3−H3d···O4_2	0.918	1.98	2.897	175.82
N3−H3a···O3_2	0.921	2.446	2.835	105.59
N3−H3d···O3_2	0.918	2.478	2.835	103.39
O6−H6d···O6_2	0.850	2.524	2.944	111.57
O6−H6d···O7_2	0.850	1.923	2.740	160.79
O6−H6c···O8	0.849	2.748	2.868	89.46
O7−H7d···Br1′_2	0.849	2.243	2.978	144.92
O8−H8d···Br1	0.850	2.203	3.037	166.71

[a] In **1**, _3 corresponds to symmetry operations "1/2 + *x*, 1/2 − *y*, 1/2 + *z*" whereas _4 corresponds to "−*x*, −*y*, −*z*". [b] Atoms situated in crystallographic special positions. [c] In **2**, _2 corresponds to symmetry operation "−*x*, −*y*, −*z*".

mixing $[H_6Bn]Br_6$ and oxydiacetate with a molar ratio 1:2 in water, adjusting the acidity to pH = 5, and allowing water to evaporate slowly for a few days.

The crystal structures of **1** and **2** have been determined by means of single-crystal X-ray diffraction analysis. Table 1 contains crystallographic data for complexes **1** and **2**, whereas Table 2 contains their selected bond distances and angles. Figure 1A,B displays their ORTEP diagrams. Complexes **1** and **2** crystallize in the monoclinic $P2_1/n$ and the triclinic $P\bar{1}$ space groups both with 2 and 1 molecules/unit cell.

The centrosymmetric cationic part of **1** can be considered as the initial $[H_6P2]^{6+}$ ligand bonded to the oxalate dianion within its macrocyclic cavity, with the inversion center situated in the middle of the oxalate C−C bond. The oxalate is placed inside the cavity so that two oxygen atoms are directed upward with regard to the plane of the cavity and the other two downward (see Figure 1A). The oxalate is located so that it has a 50.29° angle with regard to the plane defined by six N atoms of the macrocyclic ligand that can be considered to define the plane of the cavity (mathematical equations for the planes are presented as Supporting Information). The aromatic rings are parallel to one another and form an angle of 77.73° with regard to the mentioned cavity plane. The oxalate is strongly bonded to the macrocyclic ligand through electrostatic interactions and also through a network of hydrogen bonds with its carboxylate groups. Thus, O1 is hydrogen bonded to the secondary macrocyclic

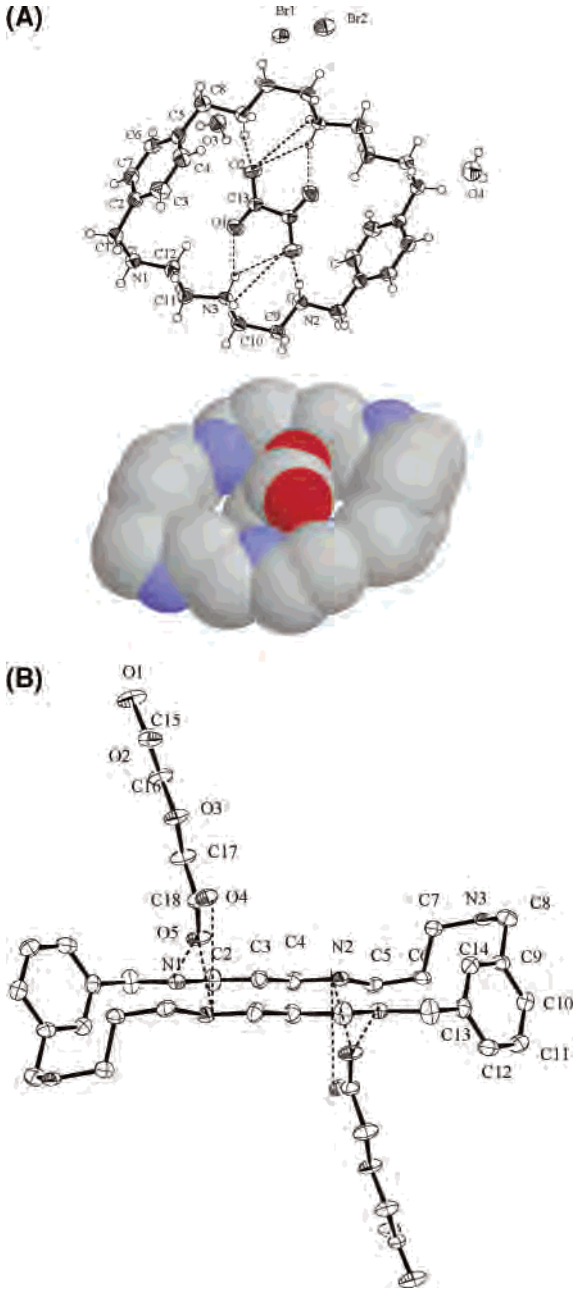

Figure 1. (A) (top) Ortep diagram (ellipsoids at 50% probability) including labeling scheme and (bottom) compact view of $[(H_6P2)(Ox)]^{4+}$. (B) Ortep diagram (ellipsoids at 50% probability) including labeling scheme of $[(H_6Bn)(Od)_2]^{2+}$.

amine N3, and O2 to N2 and N3 (see Table 2 for a complete listing of hydrogen-bonding parameters).[17] The oxalate group is not bonded to N1, but N1 is strongly hydrogen bonded to two crystallization water molecules (O3 and O4) and moderately bonded to one of the bromide counteranions, Br1. The O3 water molecule in turn is also hydrogen bonded to the oxalate anion via its oxygen atoms. The O4 molecule has four different hydrogen bonds that are situated in a tetrahedral manner and is bonding to N1 and N3 of two different but symmetrically related macrocyclic secondary

(17) (a) Taylor, R.; Kennard, O. *Acc. Chem. Res*. **1984**, *17*, 320−326. (b) Lehn, J.-M.; Meric, R.; Vigneron, J.-P.; Bkouche-Waksman, I.; Pascard, C. J. *J. Chem. Soc., Chem. Commun*. **1991**, 62.

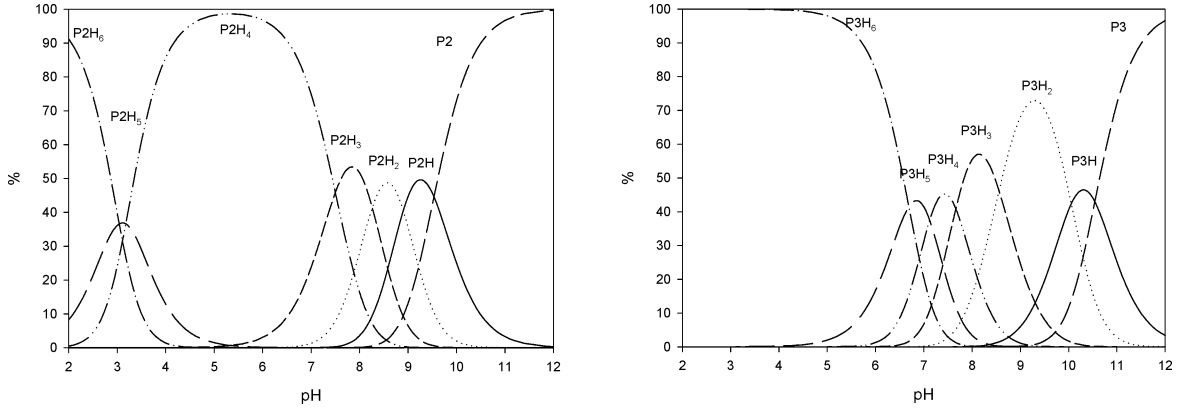

Figure 2. Species distribution diagrams for the P2 and P3 ligands a function of p[H].

amines and to two symmetrically related bromide counterions, therefore acting as bridge between symmetrically related complexes.

The centrosymmetric cationic part of **2** can be considered as the initial $[H_6Bn]^{6+}$ ligand bonded to the oxydiacetate dianion, with the inversion center situated in the center of the macrocyclic cavity. The H_6Bn moiety is forming a sort of a chair mostly flat except for the ends where the N3 secondary amines are situated up and down the main cavity plane. Thus, the two N3 atoms (N3 and its symmetry-related N3_2) are situated at the upper and lower positions with regard to the mentioned cavity plane. The aromatic rings are located nearly parallel to each other and nearly perpendicular to the cavity plane. Two oxydiacetates/macrocyclic moiety are vertically located above and below the cavity and are strongly bonded through electrostatic interactions and hydrogen bonding. This generates a pseudochain along the *x*-axis since each diacetate is bridging two symmetrically related macrocyclic moieties. The chains are interacting one another along the *y* axis through weak hydrogen-bonded water molecules that act as bridging units and along the *z* axis through hydrogen bonds between the central oxygen of the diacetate, O3, and the N3 atoms of the macrocycle (see Table 2 for quantitative values). Finally, the bromide counterions are also weakly interacting with the water molecules.

Ligands and Substrates. In this work we describe the recognition capacities of four ligands with two dicarboxylic substrates that are presented in Chart 1. The ligands are four ditopic hexaazamacroycles that differ one another in the aromatic substitution that can be *meta* or *para* and in the number of methylenic units linking the secondary amines. Thus Bd, possessing *meta* substitution and two methylenic units, is the receptor having the smallest cavity whereas P3, which possesses *para* subtitution and three methylenic units, has the largest cavity. Assuming an extended conformation of all the C and N sp^3 atoms, which is actually the conformation presented by Bn in its X-ray structure,[2,6] the relative size of their cavities can be calculated normalized to Bd, which is the ligand with the smallest cavity. In this way isomeric ligands are 12% larger in the *para* case since the cavity increases by two member ring units with respect to the *meta*; ligands with the same aromatic substitution but differing in the number of methylenic units increase their cavity size by 20%, due now to the increase in four member ring units of the cavity. From a topologic viewpoint the *meta* ligands have a rectangular shape whereas the *para* substituted are closer to a square. From the acid−base point of view the isomeric ligands have practically the same protonation constants as can be seen in Table 3[2a−c] whereas the increase in four methylenic unis increases the basicity by about 10 orders of magnitude. The species distribution diagram shown in Figure 2 for the P2 and P3 case illustrate how this difference in basicity influences the zones of predominance of the different protonated species of each ligand. Perhaps the most illustrative feature of these diagrams is that for P3 the pentaprotonated species, H_5P3^{5+}, does not start to form significantly up to pH higher than 5 whereas for P2 at pH = 2 the abundance of H_5P2^{5+} is already 9%.

Table 3. Logarithms of the Protonation Constants for Ligands (P3, Bn, P2, and Bd) and Substrates (Ox and Od) at 25.0 °C and μ = 0.10 M (KCl)

equilib[a]	P3	Bn	P2	Bd	Od	Ox
$K^H_1 = [HL]/[L][H]$	10.55	10.35	9.54	9.46	3.93	3.99
$K^H_2 = [H_2L]/[HL][H]$	10.06	9.76	8.90	8.72	2.83	1.0
$K^H_3 = [H_3L]/[H_2L][H]$	8.56	8.54	8.26	7.98		
$K^H_4 = [H_4L]/[H_3L][H]$	7.67	7.78	7.50	7.12		
$K^H_5 = [H_5L]/[H_4L][H]$	7.12	7.22	3.18	3.75		
$K^H_6 = [H_6L]/[H_5L][H]$	6.70	6.67	3.04	3.40		
$\Sigma \log K^H_i$	50.64	50.32	40.42	40.42		
$10^3\sigma_{fit}$ or ref	1.9	2.1	1.5	1.9	2.1	3.7

[a] Charges have been omitted for clarity.

The substrates used in this work are the oxalic and oxydiacetic dicarboxylic acids, and they differ in size and molecular flexibility. While oxalic acid can be considered a very rigid molecule, the oxydiacetic acid can be considered as highly flexible due to the three sp^3 atoms linking the carboxylic groups. Their protonation constants are also displayed in Table 3.[10]

Formation of Ternary Species H:L:S. With the individual protonation constants for all the ligands and substrates described in the previous section precisely known, then the potentiometric data (Figure 3A for the P2−Ox and P3−Ox systems) of a solution containing an equimolecular amount of ligand and substrate can be resolved giving the nature and log K^R values of the species generated (see Table 4).

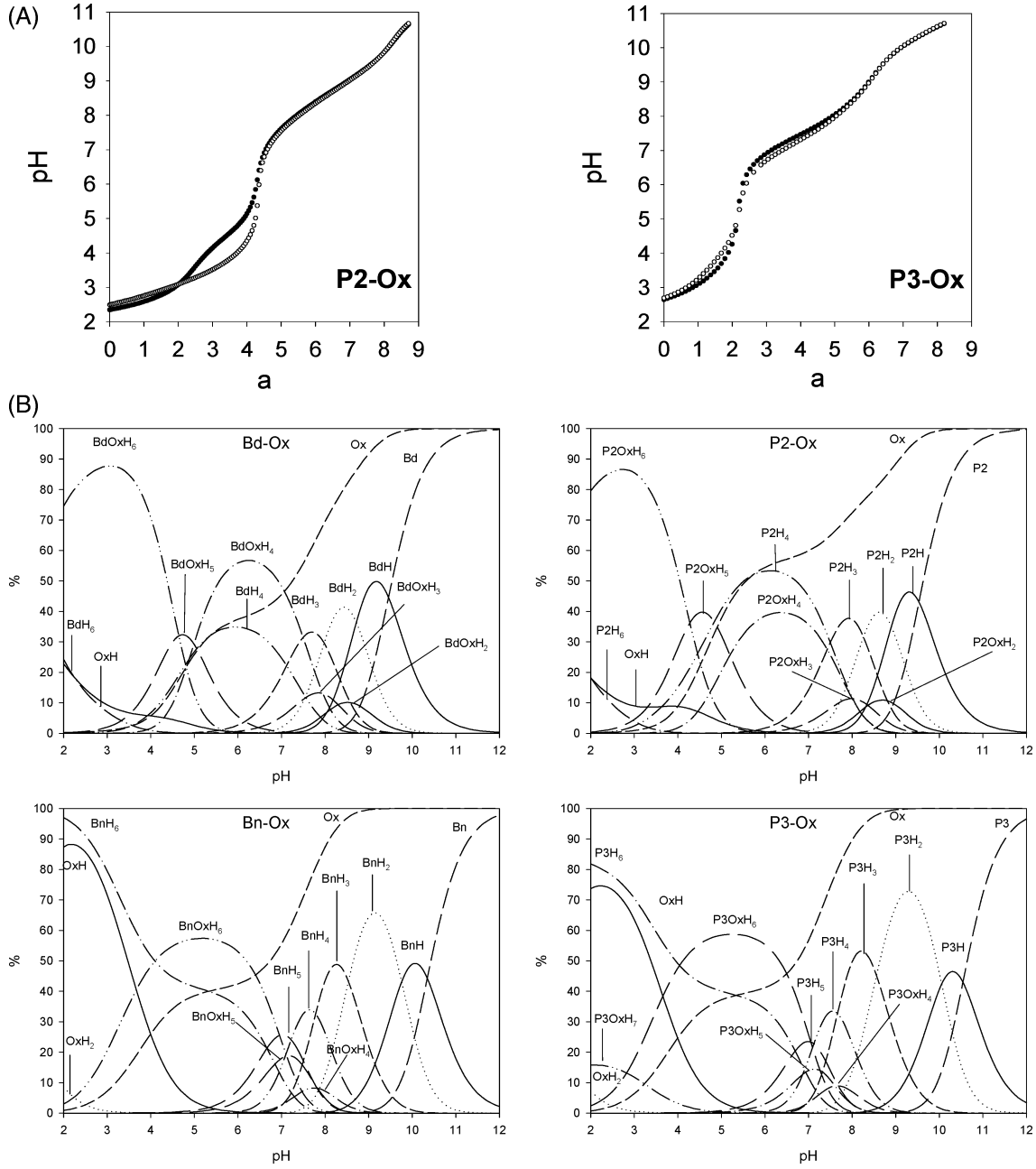

Figure 3. (A) (●) Experimental curves obtained for the potentiometric titrations of equilibrated oxalate substrate (2.0×10^{-3} M) with the ligands P2 and P3 (2.0×10^{-3} M) at 25.0 °C and $\mu = 0.1$ M (KCl) and (○) calculated potentiometric curve for the same system assuming there is no interaction between the substrate and the ligand. (B) Species distribution diagram as a function of p[H] for the four L−Ox systems (L = Bd, P2, Bn, P3).

For the P2−Ox system ($\sigma_{fit} = 0.0060$) the presence of five equilibrium species detected can be expressed as follows:

$$H_2P2^{2+} + Ox^{2-} \rightleftarrows H_2P2Ox \quad \log K^R_2 = 2.22 \qquad (1)$$

$$H_3P2^{3+} + Ox^{2-} \rightleftarrows H_3P2Ox^{+} \quad \log K^R_3 = 2.32 \qquad (2)$$

$$H_4P2^{4+} + Ox^{2-} \rightleftarrows H_4P2Ox^{2+} \quad \log K^R_4 = 2.82 \qquad (3)$$

$$H_5P2^{5+} + Ox^{2-} \rightleftarrows H_5P2Ox^{3+} \quad \log K^R_5 = 4.84 \qquad (4)$$

$$H_6P2^{6+} + Ox^{2-} \rightleftarrows H_6P2Ox^{4+} \quad \log K^R_6 = 6.08 \qquad (5)$$

Here K^R_i's are the recognition constant of protonation degree i and are listed in order of appearance from high to low p[H].

Figure 3B displays the species distribution diagrams as a function of p[H] obtained for the four L−Ox systems; the diagrams for the other four L−Od systems are relatively similar and are displayed as Supporting Information.

For the L−Ox (L = Bd and P2) systems it is interesting to note that over the p[H] range 2−7 the predominant species are H_i:L:Ox rather than the individual species derived from protonation of the ligand and substrates. This range is reduced to 4−6.5 for similar systems but using the more basic Bn and P3 ligands that contain three methylenic units. It is also worth mentioning that in all cases the more abundant species are the H_6LS; Bd and P2 reach a maximum abundance of nearly 90% at p[H] = 3.0, whereas for Bn and P3 the maximums are shifted to p[H] = 5.0 and the abundance is

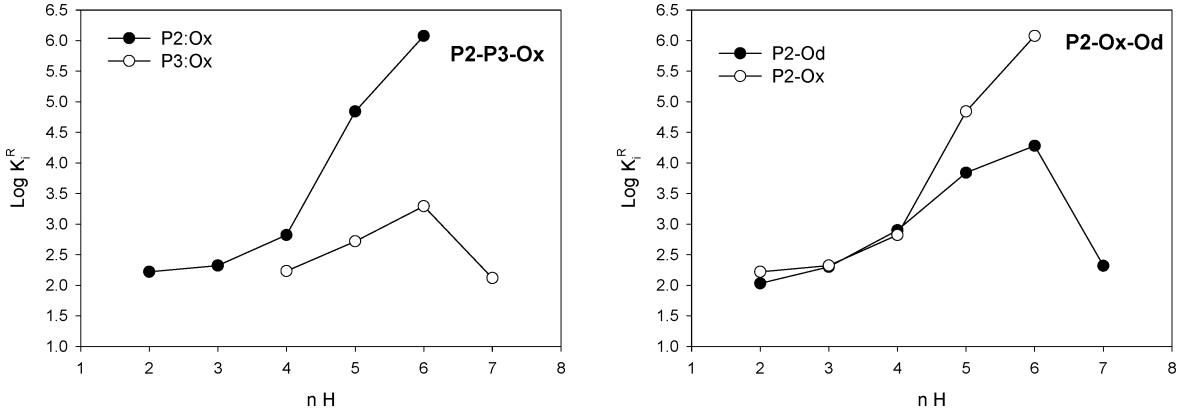

Figure 4. log K^R_i versus *n*H (the different ternary species with various degrees of protonation) for the P2−Ox/P3−Ox and P2−Ox/P2−Od systems.

Table 4. Stepwise Association Constants (*K*) for the Interaction of L (L = Bd, P2, Bn, and P3) with S (S = Ox and Od) at 25.0 °C and μ = 0.10 M (KCl)

stoich							
L	S	H	equilib[a]	Bd	P2	Bn	P3
			Oxalate (Ox)				
1	1	2	$[H_2LOx]/[H_2L][Ox]$	2.18	2.22		
1	1	3	$[H_3LOx]/[H_3L][Ox]$	2.50	2.32		
1	1	4	$[H_4LOx]/[H_4L][Ox]$	3.33	2.82	2.20	2.23
1	1	5	$[H_5LOx]/[H_5L][Ox]$	4.76	4.84	2.80	2.72
1	1	6	$[H_6LOx]/[H_6L][Ox]$	5.83	6.08	3.25	3.30
1	1	7	$[H_7LOx]/[H_6L][HOx]$				2.12
			$10^3\sigma_{fit}$	7.7	6.0	3.5	7.2
			Oxydiacetate (Od)				
1	1	1	[HLOd]/[HL][Od]	1.91		1.80	2.18
1	1	2	$[H_2LOd]/[H_2L][Od]$	2.01	2.03	1.74	2.04
1	1	3	$[H_3LOd]/[H_3L][Od]$	2.60	2.30	2.08	2.37
1	1	4	$[H_4LOd]/[H_4L][Od]$	3.28	2.90	2.42	2.53
1	1	5	$[H_5LOd]/[H_5L][Od]$	3.52	3.84	2.78	2.82
1	1	6	$[H_6LOd]/[H_6L][Od]$	4.10	4.28	3.01	2.97
1	1	7	$[H_7LOd]/[H_6L][HOd]$	2.57	2.32	2.30	2.12
1	1	8	$[H_8LOd]/[H_6L][H_2Od]$	2.48		1.90	1.56
			$10^3\sigma_{fit}$	2.8	3.8	3.6	2.8

[a] Charges have been omitted for clarity.

lowered to 60%. The highest equilibrium constant for the present ternary recognition complexes H:P2:Od described in eqs 1−5 also corresponds to the formation of the species H_6P2Ox^{4+}, log $K^R_6 = 6.08$, where Coulombic interaction and potential hydrogen bonding reach a maximum. For the H_6-$P3Ox^{4+}$ case this value is reduced to 3.30.

The recognition constant values obtained for the isomeric Bn and P3 ligands containing three methylenic units bonding the amines lay within the range of host−guest interactions with cyclic and acyclic receptors and carboxylic acids reported in the literature.[3e,18] However the recognition constants obtained for the Bd and P2 ligands with regard to the oxalate anion are the highest reported in the literature after the ones recently described by Nelson[3a] et al. using an azacryptate as a host. It also turns out that Nelson's complex and ours are the only two examples described in the literature where the evidence for the oxalate being situated within the cavity of the macrocyclic guest is also obtained by means of X-ray crystallography.

The potentiometric data was also mathematically treated by assuming a 1:2 L:S stoichiometry, given the crystalline precipitation of complex **2** containing this stoichiometry. Nevertheless in any case, no meaningful results were obtained using this stoichiometry indicating that the driving force for the formation of **2** is probably its higher insolubility than the corresponding 1:1 species.

^{1}H NMR spectroscopy was also used to follow the complexation process for the Bd−Ox and Pd−Ox systems within the pH ranges of the potentiometric titrations. The chemical shifts of all the resonances of the free ligands were found to decrease as the pH increased. Small complexation induced shifts (CIS) were also found for ligand protons, corroborating the formation of ternary species, and are graphically displayed as Supporting Information.

Competitive Diagrams and Molecular Flexibility. Figure 4 presents plots of the log K^R_i versus *n*H, for different ternary species with various degree of protonation for selected systems. Figure 5A presents competitive calculated species distribution diagrams and total species distribution diagrams for equimolecular amounts of one ligand−two substrates systems L−Ox vs L−Od whereas Figure 5B presents similar graphs for systems comparing two ligands and one oxalate.

For the Bd−Ox−Od competitive system, H:Bd:Ox species predominate over H:Bd:Od within the p[H] range 2−7, as a consequence of the higher binding constants found for the Bd−Ox system with respect to the Bd−Od system. The total species distribution diagram gives a graphical view of the selectivity of the Bd ligand for the Ox substrate with respect to Od. For instance for the Bd−Ox−Od competitive system (Figure 5A) at p[H] 3.20, 94.8% of the Bd ligand is complexed with the two substrates, 84.3% forming H:Bd:Ox species and 10.5% forming H:Bd:Od species. That implies a selectivity of 88.9% in favor of the Ox complexation against Od (the selectivity at a given p[H] for the formation of H_i:Bd:Ox species over H_i:Bd:Od is defined here as $[(\%\ H_i{:}Bd{:}Ox)/((\%\ H_i{:}Bd{:}Ox) + (\%\ H_i{:}Bd{:}Od))] \times 100$).

(18) (a) Hosseini, M. W.; Lehn, J.-M. *J. Am. Chem. Soc.* **1982**, *104*, 3525−3527. (b) Hosseini, M. W.; Lehn, J.-M. *Helv. Chim. Acta* **1986**, *69*, 587. (c) Lehn, J.-M.; Meric, R.; Vigneron, J.-P.; Waksman-Bkouche, I.; Pascard, C. J. *J. Chem. Soc., Chem. Commun.* **1991**, *62*. (d) Dietrich, B.; Hosseini, M. W.; Lehn, J.-M.; Sessions, R. B. *J. Am. Chem. Soc.* **1981**, *103*, 1282−1283. (e) Kimura, E.; Sakonaka, A.; Yatsunami, T.; Kodama, M. *J. Am. Chem. Soc.* **1981**, *103*, 3041−3049. (f) Bencini, A.; Bianchi, A.; Burguete, M. I.; García-España, E.; Luis, S. V.; Ramírez, J. A. *J. Am. Chem. Soc.* **1992**, *114*, 1919−1921. (g) Lu, Q.; Motekaitis, R. J.; Reibenspies, J. J.; Martell, A. E. *Inorg. Chem.* **1995**, *34*, 4958. (h) Motekaitis, R. J.; Martell, A. E. *Inorg. Chem.* **1996**, *35*, 4597.

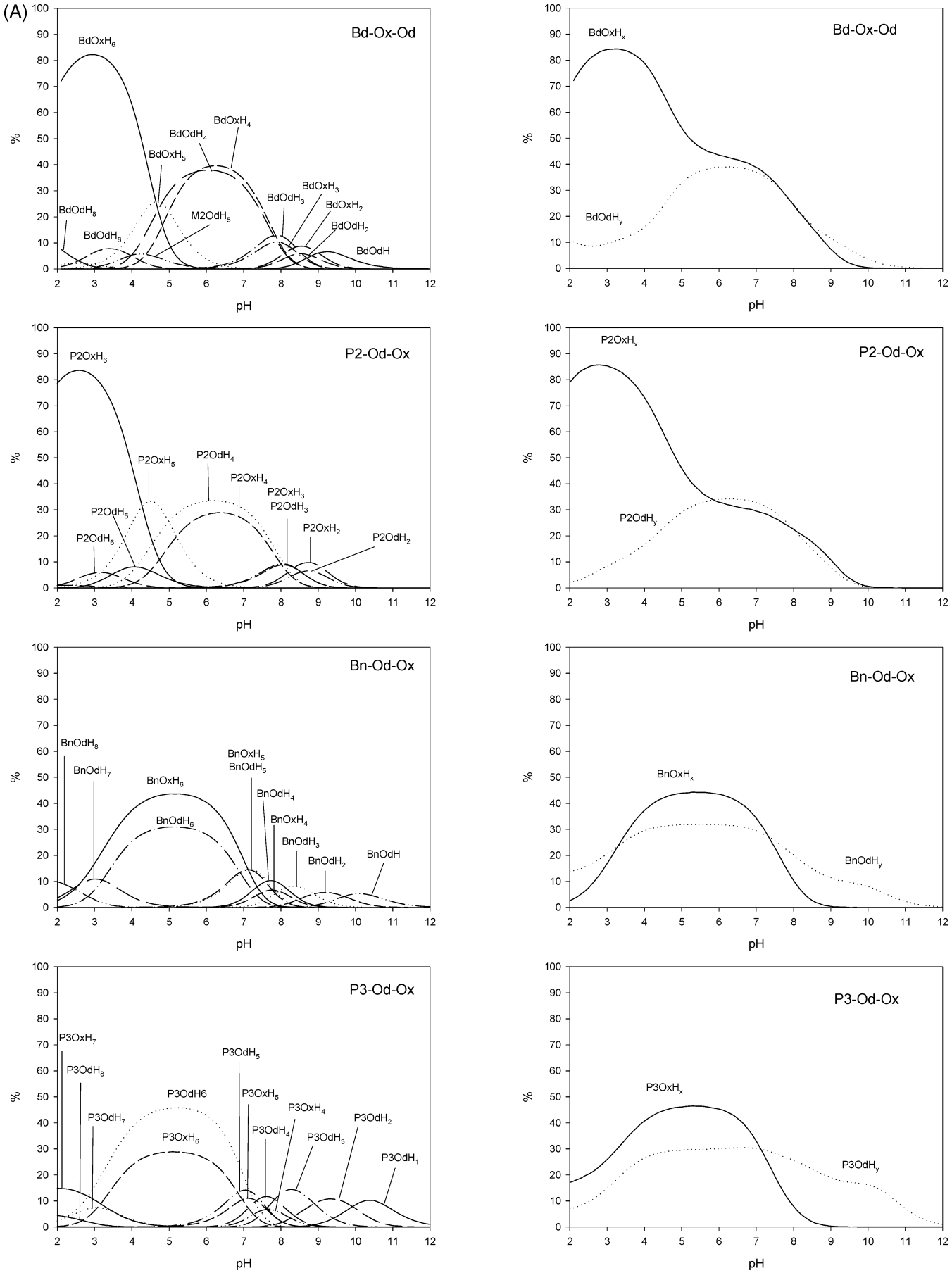
(A)
Bd-Ox-Od
BdOxH6
BdOxH4
BdOdH4
BdOxH5
BdOxH3
BdOdH3
BdOxH2
BdOdH2
BdOdH8
M2OdH5
BdOdH6
BdOdH
%
pH
Bd-Ox-Od
BdOxHx
BdOdHy
%
pH
P2-Od-Ox
P2OxH6
P2OxH5
P2OdH4
P2OxH4
P2OxH3
P2OdH3
P2OdH5
P2OxH2
P2OdH6
P2OdH2
%
pH
P2-Od-Ox
P2OxHx
P2OdHy
%
pH
Bn-Od-Ox
BnOdH8
BnOdH7
BnOxH6
BnOxH5
BnOdH5
BnOdH4
BnOxH4
BnOdH6
BnOdH3
BnOdH2
BnOdH
%
pH
Bn-Od-Ox
BnOxHx
BnOdHy
%
pH
P3-Od-Ox
P3OxH7
P3OdH8
P3OdH5
P3OdH6
P3OxH5
P3OxH4
P3OdH7
P3OdH4
P3OdH2
P3OxH6
P3OdH3
P3OdH1
%
pH
P3-Od-Ox
P3OxHx
P3OdHy
%
pH

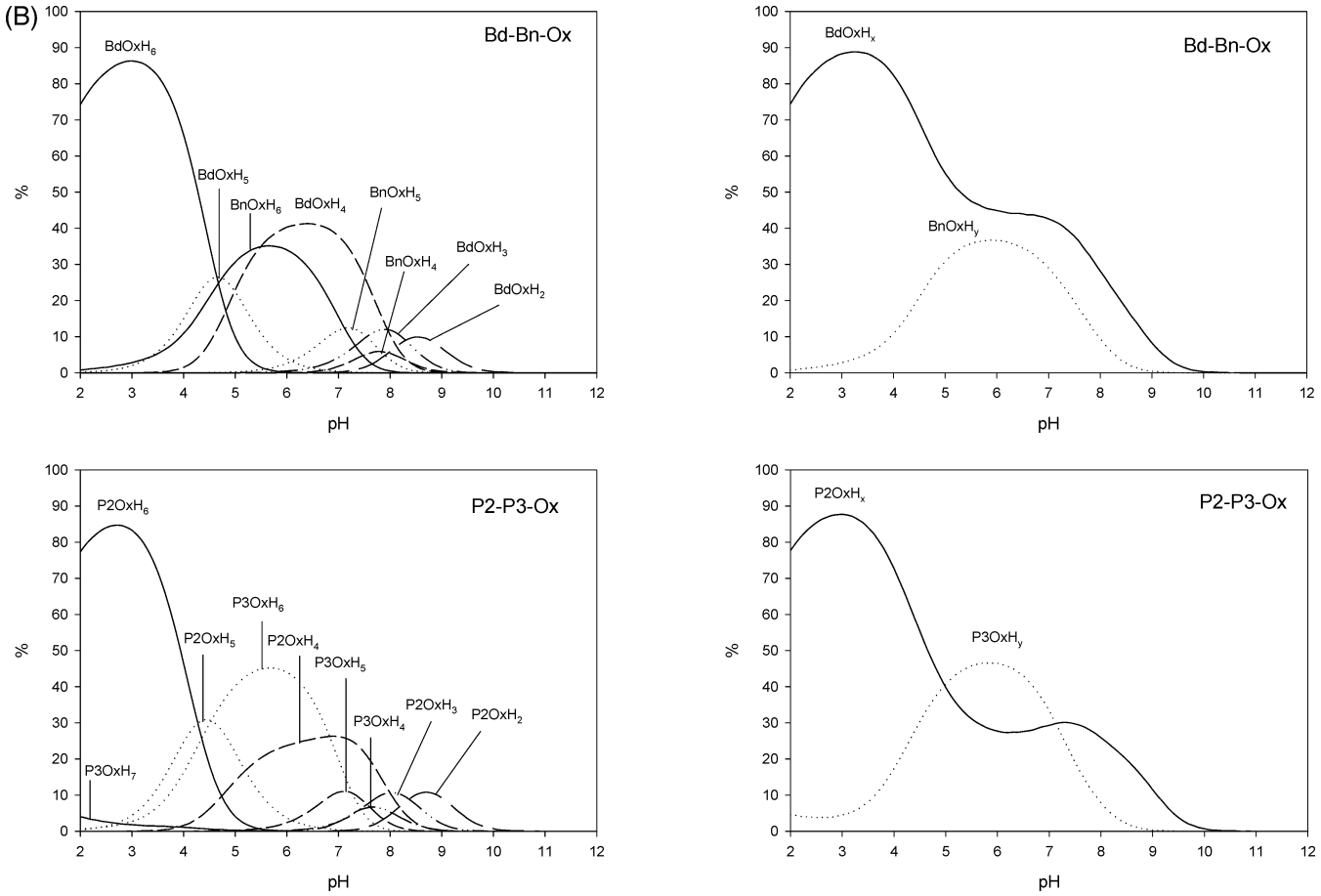

Figure 5. (A) Competitive calculated species distribution diagram and total species distribution diagrams for systems with equimolecular amounts of L−Ox−Od (Bn, Bd, P2, P3) and (B) those for Bd−Bn−Ox and P2−P3−Ox.

The P2−Ox−Od system parallels that of the Bd just described, where the P2 ligand display higher affinity for the oxalate substrate than for the oxydiacetate, which is also shown graphically in Figure 4. A quantitative analysis can be carried out calculating the $\Delta\log K^{R}_{6}$ defined as

$$\Delta\log K^{R}_{6} = \log K^{R}_{6}(H_6LS) - \log K^{R}_{6}(H_6LS') \qquad (6)$$

for a particular ligand and two different substrates (S and S′). For the P2−Ox−Od system the $\Delta\log K^{R}_{6} = 1.80$ (1.73 for Bd). The stronger affinity of Ox over Od for either the P2 or Bd ligand receptors is attributed to the fact that the Ox is capable to better accommodate into the macrocyclic cavity of the ligand than Od and its rigidity produces an even stronger Coulombic and hydrogen-bonding interactions. This adequate fit of the oxalate with regard the P2 cavity is further corroborated by X-ray diffraction analysis as has been shown in a previous section.

When a comparison is made of the behavior of oxalate with the two isomeric ligands P2 and Bd, it is found that the affinities are relatively similar. This means that different cavity topology presented by the Bd (rectangular) and P2 (squared) does not substantially affect the overall bonding. This can be understood if one takes into consideration, that as shown in the X-ray structure (see Figure 1A), the oxalate due to its rigidity only binds to the ligand receptor through four of the six secondary amines. Given the relative flexibility of the ligand receptors, the *four-way* bonding can take place with comparable restrains for the two isomers and thus bind in a very similar manner.

For the Bn−Ox−Od and P3−Ox−Od competitive systems, depicted in Figure 5A, the behavior parallels that of their analogous ligands bearing only two methylenic units within secondary amines Bd and P2, respectively, but with a lower degree of differentiation. This is clearly observed in a quantitative fashion calculating $\Delta\log K^{R}_{6}$, which now turns out to be 0.33 for the P3 ligand receptor (0.24 for Bn). This decrease in recognition capacity is due to an increase of the macrocyclic cavity dimension of the Bn and P3 ligands that produces a much poorer fit.

Finally, the less basic ligands containing two methylenic units Bd ($\log \beta^{H}_{6} = 40.42$) and P2 (40.42) bind stronger to the substrates than those containing three methylenic units Bn (50.32) and P3 (50.64). This is seen numerically comparing the stepwise recognition constant values of Table 4 and graphically in Figure 4 and in the competitive diagrams of Figure 5b where it can be observed that H:P2:Ox predominates over a much larger p[H] range than the corresponding H:P3:Ox. The corresponding $\Delta\log K^{R}_{6}$ values are 2.78 for the P2 vs P3 case and 2.58 for the Bd vs Bn case. This produces p[H] zones where the selectivity of one ligand for a substrate is very high, as shown for instance in Figure 5B where at pH = 3.3 the selectivity of the Bd ligand

over Bn for the oxalate substrate is 95.6%. This behavior had previously been observed for similar ligands but interacting with phosphate and nucleotide type substrates.[2a,b]

In conclusion, the results reported here show that the appropriate ligand design allows to modulate the topology and flexibility of a receptors cavity and thus allows one built up tailored molecules for specific substrates. In this particular case it has been shown how the appropriate hexaazamacrocyclic ligand, under the right conditions, can strongly and selectively bind to oxalate, a rigid substrate, and generate much weaker interactions with another flexible dicarboxylic acid like oxydiacetic.

Acknowledgment. This research has also been financed by the MCYT of Spain through Project BQU2000-0458. A.L. is grateful to the CIRIT Generalitat de Catalunya (Spain) for the Distinction Award and the Aid SGR2001-UG-291. C.A. thanks the University of Girona for the allocation of a doctoral grant.

Note Added after ASAP: Figure 5A was missing from the version of this paper posted ASAP on March 17, 2004. The corrected version appeared on April 1, 2004.

Supporting Information Available: CIF files for complexes **1** and **2** together with structural parameters, species distribution diagrams, and NMR details. This material is available free of charge via the Internet at http://pubs.acs.org.

IC035121P